Biogeochemistry (2021) 156:131–143
https://doi.org/10.1007/s10533-021-00774-y

Mechanisms influencing physically sequestered soil carbon in temperate restored grasslands in South Africa and North America

Drew A. Scott · Elizabeth M. Bach · Chris C. Du Preez · Johan Six · Sara G. Baer

Received: 12 May 2020 / Accepted: 23 February 2021 / Published online: 11 March 2021

Abstract Sequestering carbon (C) into stable soil pools has potential to mitigate increasing atmospheric carbon dioxide concentrations. Carbon accrues in grassland soil restored from cultivation, but the amount of physically protected C (here measured as microaggregate-within-macroaggregate C) and predominant mechanisms of accrual are not well understood. We modeled the rate of physically protected carbon accrued in three mesic temperate perennial restored grasslands from cross-continental regions using datasets with a wide range of restoration ages from northeast Kansas, USA; southeast Nebraska, USA; and northeast Free State, South Africa. Further, we investigated major controls on the amount of physically protected C in each site using structural equation modeling. Variables in the structural equation model were root biomass, root C:N ratio, soil structure (indicated by bulk density, percent of macroaggregates on a per whole soil mass basis, and percent of microaggregate-within-macroaggregates on a per macroaggregate mass basis), microbial composition (indicated by microbial biomass C, total phospholipid fatty acid [PLFA] biomass, and PLFA biomass of arbuscular mycorrhizae fungi [AMF] biomass), and microaggregate-within-macroaggregate C on a per whole soil mass basis. Across all sites, physically protected C accrued at a rate of 16 ± 5 g m^{-2} $year^{-1}$. Data from South Africa fit an *a priori* metamodel developed for northeast KS that hypothesized physically protected C could be explained as a function of microbial composition, soil structure, root C:N ratio,

Responsible Editor: William R. Wieder.

Supplementary Information The online version contains supplementary material available at https://doi.org/10.1007/s10533-021-00774-y.

D. A. Scott (✉)
Ronin Institute, 127 Haddon Pl, Montclair, NJ, USA
e-mail: drew.scott@ronininstitute.org

E. M. Bach
The Nature Conservancy, Nachusa Grasslands, 8772 S Lowden Rd, Franklin Grove, IL 61031, USA

C. C. Du Preez
Department of Soil, Crop and Climate Sciences, University of the Free State, Nelson Mandela Dr, Bloemfontein 9301, South Africa

J. Six
Department of Environmental Systems Science, ETH Zurich, Universitätstrasse 2, 8092 Zurich, Switzerland

S. G. Baer
Department of Ecology and Evolutionary Biology, Kansas Biological Survey, University of Kansas, Lawrence, KS, USA

and root biomass (listed in order of strength of direct effect on physically protected C). In contrast to the model-based hypothesis, root C:N ratio was the strongest influence (negative) on physically protected C in South Africa. The lesser effect of AMF on physically protected C in South Africa was consistent with lower AMF biomass in arid environments. The hypothesized model did not fit southeast Nebraska data possibly due to high ($\sim$ 30%) clay content. Overall, these results suggest that physically protected C in soil with moderate amounts of clay (more than 10% and less than 30%) can be predicted with knowledge of roots (biomass and C:N ratio), microbial biomass, and soil aggregation.

Keywords Arbuscular mycorrhizal fungi · Conservation Reserve Program · Microaggregate-within-macroaggregate · Microbial biomass · Roots · Soil organic matter · Soil structure

Introduction

Diverse solutions are required to address the global need to reduce carbon dioxide concentrations in atmosphere through sequestration into long-term stable pools. Restoring cultivated land back to native grassland habitat presents an opportunity to accrue and sequester atmospheric carbon (C) into stable soil organic matter pools (Baer and Birgé 2019). Because cultivated soils have an organic C saturation deficit [lower organic C storage than soils' capacity to store C (reviewed by Stewart et al. 2007)], these soils have capacity to accrue organic C once tillage is ceased and C inputs from perennial plants exceed decomposition. Restoring cultivated land to grassland has been shown to increase total soil C pools (Jastrow 1996; Baer et al. 2002, 2003, 2010, 2015; Scott et al. 2017), but estimates of total soil C accrual from this practice vary widely (McLauchlan 2006) and our understanding of factors controlling C accrual and protection in soil is incomplete. Variation in observed rates and magnitude of soil C accrual in restored grasslands around the world limits our ability to understand primary (and secondary) drivers responsible for building soil C. While strong variation across global grasslands is expected, knowledge of consistent underlying mechanisms and sources of variation in realized responses can improve restoration and management decisions to assure, or even improve, soil C accrual and storage.

Increasing C in soil during grassland restoration coincides with concomitant changes in several physical, chemical, and biological soil properties that influence different protection mechanisms of C in soil. Physico-chemical protection of C in soil results when soil minerals arranged around organic matter inhibit oxidation (Paustian et al. 1997; Six et al. 2004). Minerals associated with soil organic matter form a hierarchical aggregate structure (Tisdall and Oades 1982; Elliot et al. 1984) and C contained in microaggregates-within-macroaggregates is considered a diagnostic fraction of sequestered C in soil (Denef et al. 2004; 2007; Kong et al. 2005; Six and Paustian 2014). Microaggregate-associated C can persist for a few centuries in soil, though land management and clay minerology greatly influence mean residence time (Six et al. 2002). Microaggregate-within-macroaggregate formation is associated with slower macroaggregate turnover and therefore more physical protection of organic matter (Six et al. 2000b). Biologically, increases in root biomass, microbial biomass, and fungi:bacteria ratio during grassland restoration on formerly cultivated soil facilitate recovery of a hierarchical aggregate structure indicated by increases in mean aggregate diameter and decreases in bulk density (Jastrow 1996; Matamala et al. 2008; Bach et al. 2010; Baer et al. 2010, 2015; Rosenzweig et al. 2016; Scott et al. 2017). Structural equation modeling allows for multivariate examination of the relative strength of these dynamically changing biogeochemical factors on soil C accrual and resultant model presents a mechanistic hypothesis on causal influence of multiple factors on soil C accrual during grassland restoration.

We previously used structural equation modeling to examine multiple biogeochemical factors' collective and relative influence on the accrual of microaggregate-within-macroaggregate C during grassland restoration in Kansas, USA (Scott et al. 2017). The structural equation model included several factors known to influence physically sequestered C (root biomass, root quality, microbial biomass, aggregate distribution, and aggregate C) based on the following causal relationships. Root biomass (inputs) and quality (indicated by C:N ratio [wider ratio indicating less decomposable]) have direct positive effects on microaggregate-within-macroaggregate C (i.e. increasing root inputs and C:N lead to greater microaggregate-within-macroaggregate C; Robinson

and Jacques 1958; Gale et al. 2000; Puget and Drinkwater 2001; Six et al. 2004). Root biomass and quality also have positive indirect effects on microaggregate-within-macroaggregate C through their influence on development of microbial biomass (Elliot et al. 1984; Newman 1985; Smucker and Safir 1986) and recovery of soil structure (Scott 1998; Angers and Caron 1998; Ehrenfeld et al. 2005). Microbial biomass and composition influences microaggregate-within-macroaggregate C via recalcitrance of necromass, with fungi generally producing less decomposable necromass compared to bacteria (Simpson et al. 2004). As such, microbial biomass, fungi:bacteria ratio within aggregates, and soil structure are correlated because biological binding agents promote aggregate formation and stability (reviewed in Six et al. 2004; Ehrenfeld et al. 2005; Wilson et al. 2009; Smith et al. 2014).

These mechanisms driving physically protected C have been shown to apply over a range of restoration ages in independent or two-site comparative studies, but generality has not been demonstrated using studies conducted across multiple regions. When the mechanisms controlling physically protected soil C across a chronosequence of restorations in Kansas were evaluated simultaneously using structural equation modeling, the influence of some variables became negligible. Scott et al. (2017) found that their model predicted microbial composition (indicated by microbial biomass C, phospholipid fatty acid [PLFA] biomass of arbuscular mycorrhizal fungi [AMF], and PLFA biomass of all other major microbial groups) to be the strongest direct path to microaggregate-within-macroaggregate C (positive effect). The second strongest direct path was soil structure (positive effect; indicated by bulk density, macroaggregate percentage by weight, and microaggregate-within-macroaggregate percentage by weight; Fig. 1). Root biomass and root C:N ratio had negligible causal influence on aggregate-protected C. This model proved to be highly accurate at predicting microaggregate-within-macroaggregate C for the Flint Hills region of tallgrass prairie.

Building from the model results of Scott et al. (2017), here we explore the generality of the causal influences on physically protected C in restored soils that varied in time since sown to native grasses (restoration age) by including two additional chronosequences from different cross-continental

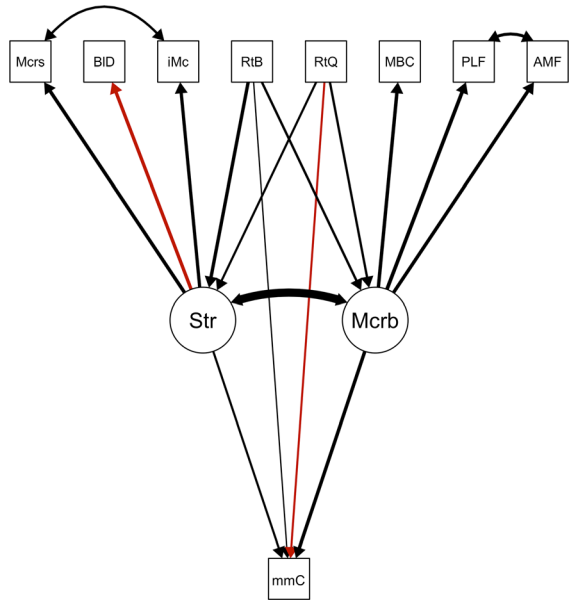

Fig. 1 SEM hypothesized of strength of causal influences on physically protected carbon, adapted from Scott et al. (2017). Line width correlates with path strength. Single-headed arrows indicate causal relationships; double-headed arrows represent correlations. Red paths indicate negative relationships; black paths represent positive relationships. Abbreviations for soil properties in this figure are kept the same as the original publication: *Mcrs* percentage of macroaggregates by mass; *BlD* bulk density; *iMc* percentage of microaggregates-within-macroaggregates by mass; *Str* soil structure (latent variable indicated by percent microaggregates-within-macroaggregates by mass, percent macroaggregates by mass, and bulk density); *RtB* root biomass; *RtQ* root quality (C/N ratio); *MBC* microbial biomass C; *PLF* total phospholipid fatty acid biomass; *AMF* phospholipid fatty acid biomass of arbuscular mycorrhizal fungi; *Mcrb* microbial composition (latent variable indicated by total PLFA biomass, PLFA biomass of AMF, and microbial biomass C); *mmC* microaggregates-within-macroaggregates C

regions. All fields were sampled using the same methods. We examined the fit of data from mesic temperate perennial restored grasslands in northeast Free State, South Africa (NEFS) and southeast Nebraska, USA (SENE), and a combined dataset including all three sites. We hypothesized that the physically protected C pool (microaggregate-within-macroaggregate C would increase linearly with restoration age and C sequestration in soil is a generalizable ecosystem response to grassland restoration in soils with adequate and similar clay content. We also hypothesized that microbial biomass and composition (PLFA biomass of AMF and all other major microbial groups) will explain most variation in

the microaggregate-within-macroaggregate C pool across all sites.

Methods

Site descriptions

All chronosequences used in this analysis were selected based on the criteria that sites had been cultivated long enough to approach or reach new (lower) equilibrium C stocks. Previous work described an exponential decline to lower equilibrium following 34 years of cultivation (Du Toit et al. 1994; Lobe et al. 2002). All restorations were planted to perennial C_4 grasses, and contained at least 9% clay, as grasslands restored on soil with little to no clay content do not accrue C on a decadal time scale (Baer et al. 2010). All chronosequences included a decadal range of restoration ages.

The southeast Nebraska, USA (SENE) site consisted of 22 independent restorations that were part of the United States Department of Agriculture's Conservation Reserve Program, with ages ranging from 4 to 19 years restored. These restorations were on silty clay loam (Fine smectitic, mesic Aquertic Argiudolls) soils formed by loess with 0–6% slope. Clay content of these soils ranged from 23 to 39% (mean = 33%). Inorganic C was not quantified for these soils but is likely a small pool as A and B horizons of typic pedons for this family are acidic (USDA 2008, 2020). Crop rotations in this area often include corn, wheat, oat, soy, and sorghum. These fields were cultivated for more than 20 years. Most of these fields were restored by sowing equal amounts of 6 grass species (*Andropogon gerardii* Vitman, *Schizachyrium scoparium* (Michx.) Nash, *Panicum virgatum* L., *Pascopyrum smithii* (Rydb.) Á. Löve, *Bouteloua curtipendula* (Michx.) Torr., and *Sorghastrum nutans* (L.) Nash). This region had a mean annual temperature of 10.9 °C and a mean annual precipitation of 757 mm. Baer et al. (2010) and Bach et al. (2010) provide a detailed description of the fields sampled in this chronosequence. Specific locations are not available because these fields are on private property.

The northeast Kansas, USA (NEKS) site consisted of 6 independent restorations, with ages ranging from 1 to 35 years restored. The 35-year-old restoration was on a Clime silty clay loam (fine, mixed, active, mesic Udorthentic Haplustolls)-Sogn silt loam complex (loamy, mixed, superactive, mesic Lithic Haplustolls) soils formed from weathered shale and limestone respectively. The other NEKS restorations were on Reading silt loam (fine silt, mixed, superactive, mesic Pachic Argiudolls) soils formed from alluvial silt deposits. Sampled areas had less than 5% slope. Clay content of these soils ranged from 24 to 33 (mean = 30%). Soil pH (1:1 soil:distilled water by weight) ranged from 5.6 to 7.5 (Rosenzweig et al. 2016). Inorganic C in the top 10 cm was low across all fields (average of 0.1% of soil mass and 6% of total carbon; Scott et al. 2017). These fields were in cultivation for 50 or more years prior to restoration. Crop rotations in this area often include corn, soy, sorghum, and winter wheat. These fields were restored by sowing a variety of seed mixes. The most commonly encountered plant species were *Andropogon gerardii* Vitman, *Sorghastrum nutans* (L.) Nash, and *Lespedeza capitate* Michx. This site had a mean annual temperature of 12.7° C and a mean annual precipitation of 833 mm. Scott et al. (2017) provide a detailed description of the fields sampled in this chronosequence; a map is included in Scott et al. (2019).

The northeast Free State, South Africa (NEFS) site consisted of 17 independent restorations near Harrismith, with restoration ages ranging from 4 to 44 years. These restorations were on fine loamy sand to fine sandy loam, thermic, mixed Typic Plinthustalfs with less than 5% slope. Clay content of these soils ranged from 9 to 32% (mean = 18%). No inorganic C was detectable in the top 40 cm of these soils (Lobe et al. 2001). The fields were in cultivation for 30 or more years before restoration. Crop rotations in this area often include fallow, wheat, corn, and sunflower. Most fields were restored by sowing *Eragrostis curvula* (Schrad.) Nees. This site had a mean annual temperature of 13.8 °C and a mean annual precipitation of 635 mm. Baer et al. (2015) provide a detailed description of the fields sampled in this chronosequence; a map is included in Lobe et al. (2001).

Measurements

We used measurements of root biomass, root C:N ratio, soil structure (bulk density, percent of macroaggregates on a per whole soil mass basis, and percent of microaggregate-within-macroaggregates on a per macroaggregate mass basis), microbial composition

(microbial biomass C, total PLFA biomass [excluding AMF], and PLFA AMF biomass), and microaggregate-within-macroaggregate C on a per whole soil mass basis from the perennial grassland restoration chronosequences in SENE (Bach et al. 2010; Baer et al. 2010), NEFS (Baer et al. 2015), and NEKS (Scott et al. 2017). All data were collected using the same methods, with the exception of sample depth increments. Data from Scott et al. (2017) and Baer et al. (2010) were derived from 0 to 10 cm soil depth. Data from Baer et al. (2015) collected in NEFS were derived from the 0–5 cm and 5–10 cm depth. The sequestered soil carbon (represented by the microaggregate-within-macroaggregate fraction) were not previously reported for the SENE and NEFS sites.

At all sites, intact soil cores (5 cm dia., 10 cm depth [NEFS samples were divided into 0–5 and 5–10 cm depths]) were removed and stored at 4 °C until processed (within one week of sampling). In the laboratory, each core was broken along planes of natural weakness and passed through an 8 mm sieve. Gravel was removed when encountered, but most samples had no gravel. Large roots were then removed with forceps from the entire sample. Fine roots (appearing to be less than 1 mm diameter) were thoroughly picked from a quarter of the sample. Roots were washed with deionized water and dried (60°C) to determine root biomass. Dried roots and 5–10 g of soil were analyzed for %C and %N by dry combustion followed by gas chromatography on a CN Analyzer (Thermo Scientific, New Brunswick, NJ USA). A subsample of freshly sieved soil (8 mm; ~20 g) was used to determine gravimetric water content and back-calculate bulk density (g m^{-3}) based on the volume and dry weight of soil. Another subsample of freshly sieved soil (30 mL) was frozen in a falcon tube and later used for PLFA analyses. A subsample of ~ 100 g was air dried and used for aggregate fractionation.

Phospholipid fatty acid biomarkers were extracted from soils using a 1:2:0.8 chloroform/methanol/phosphate buffer extraction (Bligh and Dyer 1959; Bossio et al. 1998; DeGrood et al. 2005). Chloroform and phosphate buffer were added to the extractant to allow phase separation. The chloroform phase was retained and evaporated under N_2 gas. Solid phase extraction was used to separate the neutral- and glycolipids from the phospholipids. Fatty acid methyl esters were dissolved in hexane and analyzed with gas chromatography. See previous publications for full details (SENE: Baer et al. 2010; Bach et al. 2010; NEFS: Baer et al. 2015; NEKS: Scott et al. 2017).

A hierarchical wet-sieving method was used to fractionate soil into aggregate classes and further isolate microaggregates-within-macroaggregates according to Six et al. (2000a, b). Briefly, soil passing through an 8 mm sieve was air dried before slaking (rapidly re-wetting) and isolating aggregates (> 2 mm: macroaggregates; <2 mm and > 250 μm: small macroaggregates; <250 μm and > 50 μm: microaggregates; and < 50 μm: silt and clay). This isolation was accomplished by sequentially hand-sieving soil in a water basin at 100 back and forth motions in one minute. Soil separated by a sieve was back washed into aluminum pans and the remaining soil water mixture was poured onto the next sieve. A series of 2mm, 250 μm, and 50 μm sieves were used to isolate aggregate fractions. These aggregate fractions were dried at 60 °C. Large macroaggregates and small macroaggregate subsamples in proportional amounts were then shaken in water on a fine mesh with 50 4-mm ball bearings. The mesh isolated particulate organic matter within the macroaggregates. The water was then poured over a 50 μm sieve to isolate microaggregates-within-macroaggregates. This fraction was dried at 60 °C, then analyzed for %C and %N using the same methods described for root biomass and whole soil. Carbon stocks for this fraction and bulk soil (total C stocks) were calculated using minimum equivalent mass (average of three lowest bulk densities among all fields within a site was used for all calculation; Lee et al. 2009). In the case of NEKS total C stocks were calculated as the sum of C in aggregate fractions. Carbonates were present in small amounts, but consistent within a chronosequence such that increasing total soil C is due to organic soil C accrual. See previous publications for full details (SENE: Baer et al. 2010; Bach et al. 2010; NEFS: Baer et al. 2015; NEKS: Scott et al. 2017).

Statistical analyses

All statistics were performed with R statistical software (R Core Team 2016). Microaggregate-within-macroaggregate C and proportion of microaggregate-within-macroaggregate C responses to restoration age (fixed predictor) and location (block effect) was fit to a linear mixed model using the *lmer* function with

restricted maximum likelihood in the lme4 package (Bates et al. 2015). The NEKS dataset, which included within-field samples, was averaged to the field level to be comparable to the SENE and NEFS sites. Significance of microaggregate-within-macroaggregate C, total soil C, and proportion of microaggregate-within-macroaggregate C (microaggregate-within-macroaggregate C/total soil C) responses to restoration age were calculated using Satterthwaite's denominator degrees of freedom and Type III sum of squares with the lmerTest package (Kuznetsova et al. 2016). Conditional pseudo R^2 values were calculated using the *r.squaredGLMM* function in the package MuMIn (Bartoń 2018). Normal bootstrap confidence intervals (95%) were calculated using the package boot (Davidson and Hinkley 1997; Canty and Ripley 2017). Pearson and Spearman correlation analyses were used to assess the correlation of microaggregate-within-macroaggregate C and total soil C. Clay content, root C:N ratio, and microbial properties were compared among sites with ANOVA and least significant difference contrasts using the emmeans package (Lenth 2020). All linear models met the assumptions of homoskedasticity and normality of residuals.

Structural equation modeling has tremendous value for identifying predominant mechanisms by evaluating potential causal relationships simultaneously, though a large amount of *a priori* knowledge is needed. To test multiple potential controls on physically protected C (measured in g m^{-2}), data from all sites (NEKS, SENE, and NEFS) were combined and fit to a structural equation model (SEM) slightly modified from the model-based hypothesis presented by Scott et al. (2017; Fig. 1) that included clay content having an influence on soil structure. This clay effect on soil structure path was included to allow comparison between sites; correlation between indicators of latent variables were also removed because there was less correlation among these variables in the data. Indicators of the latent variable microbial composition were also modified from the original model. The PLFA biomass of all major microbial groups except AMF (which is a separate indicator of microbial composition), rather than total PLFA biomass was used so that a correlation could be removed from the model. Reciprocal effects of soil structure and microbial composition rather than an unexamined correlation were also used in the modified model. Model fitting was accomplished using the *sem* function in the lavaan package in R (Rosseel 2012), where a P-value based on a Chi-squared test was used to evaluate overall model fit ($P > 0.05$ considered a good fit; Grace 2006). Maximum likelihood was used in SEM models to minimize erroneous path estimates due to negative variance estimates of some variables (Grace, 2006). Standardized (for all variables) path coefficients (r) are reported for models with good overall fit; non-significant paths were denoted with N.S. Path values greater than 1 are possible because latent constructs were used in the model.

Results

Across all sites, microaggregate-within-macroaggregate C increased at a rate of 16 ± 5 g m^{-2} $year^{-1}$ (estimated marginal mean ± standard error) with a conditional pseudo R^2 value of 0.59 (Fig. 2a). Similarly, total C increased at a rate of 18 ± 7 g m^{-2} $year^{-1}$ (estimated marginal mean ± standard error) across all sites with a conditional pseudo R^2 of 0.17 (Fig. 2b). There was a strong correlation between physically protected C and total soil C (Pearson correlation = 0.62, $P < 0.001$; Spearman correlation = 0.65, $P < 0.001$). Proportion of microaggregates-within-macroaggregates (physically protected) C increased at a rate of 0.0053 ± 0.0014 $year^{-1}$ (estimated marginal mean ± standard error) with a conditional pseudo R^2 value of 0.74 (Fig. 2c). At the onset of restoration, 30% of C was in the physically protected fraction; after 44 years of restoration, 53% of C was in the physically protected fraction (Fig. 2c).

The NEFS dataset (Fig. 3) had a significant fit (χ^2 test: $P = 0.100$) to the model proposed in Scott et al. (2017), but variation in SENE (χ^2 test: $P = 0.001$) and all combined chronosequence (χ^2 test: $P < 0.001$) datasets were not as well explained. A model with NEKS and NEFS datasets combined did not converge. Because the NEFS model had a good overall fit, standardized path values were compared as a measure of effect size even if individual paths were non-significant. Unstandardized path values, unstandardized intercepts, and standardized path values for the NEFS and NEKS models are in Table 1. Standardized path values of direct effects on physically protected C in the two significant models were graphically compared in Fig. 4a; z statistics (unstandardized estimate divided by standard error) are compared in Fig. 4b,

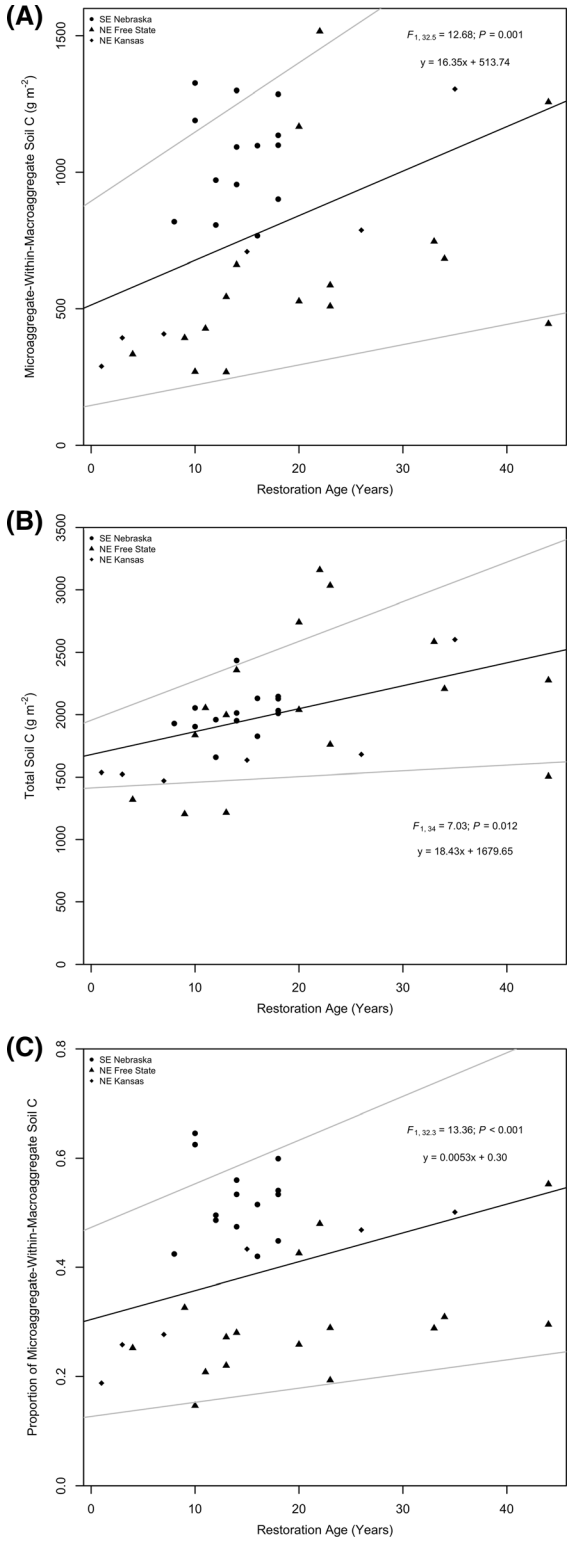

◀**Fig. 2** Microaggregate-within-macroaggregate C with restoration age (**a**), total soil C (**b**), and proportion of microaggregate-within-macroaggregate C (microaggregate-within-macroaggregate C/total soil C) (**c**). The black lines represent the fixed effect from a linear mixed model where site is a block effect. Grey lines indicate 95% confidence intervals based on normal bootstraps. Sites are indicated by point shapes

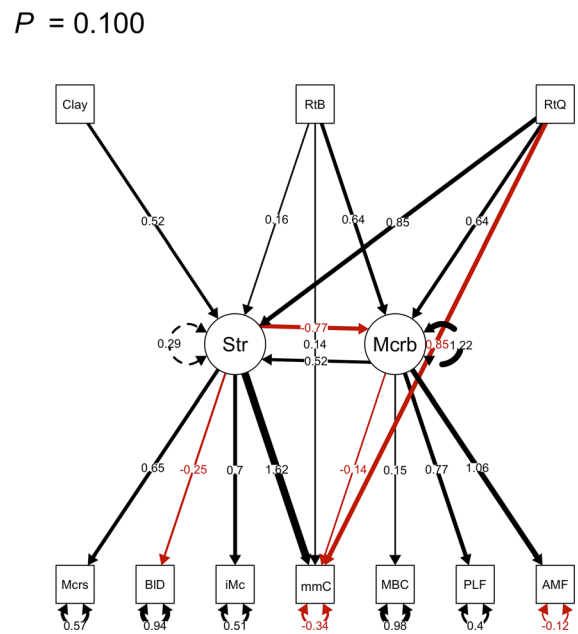

Fig. 3 Supporting SEM of factors influencing physically sequestered C in northeast Free State (NEFS), South Africa restorations. Chi-squared *P* values indicate overall model fit, where P > 0.05 is a good fit. Standardized path values are on arrows. Line width correlates with path strength. Single-headed arrows indicate causal relationships. Red paths indicate negative relationships; black paths represent positive relationships. *Mcrs* percentage of macroaggregates by mass; *BlD* bulk density; *iMc* percentage of microaggregates-within-macroaggregates by mass; *Str* soil structure (latent variable indicated by percent microaggregates-within-macroaggregates by mass, percent macroaggregates by mass, and bulk density); *RtB* root biomass; *RtQ* root quality (C/N ratio); *MBC* microbial biomass C; *PLF* total phospholipid fatty acid biomass; *AMF* phospholipid fatty acid biomass of arbuscular mycorrhizal fungi; *Mcrb* microbial composition (latent variable indicated by total PLFA biomass, PLFA biomass of AMF, and microbial biomass C); mmC, soil microaggregates-within-macroaggregates C. The following variables were transformed so that variances differed by less than a factor of 1000: Mcrs (multiplied by 10), BID (multiplied by 100), PLF (divided by 10), SIC (divided by 100), and MBC (divided by 100)

representing strength of influenced penalized by variability.

In the NEFS model (Fig. 3), the best indicator of the latent variable indicating microbial composition was PLFA biomass of AMF (r = 1.06), followed by PLFA biomass of all major microbial groups except AMF (r = 0.77), and then by microbial biomass C (r = 0.15 N.S.). The best indicator of soil structure was % microaggregates-within-macroaggregates by mass (r = 0.70), followed by % macroaggregates by mass (r = 0.65) and bulk density (r = − 0.25 N.S.). Indirect paths through the latent variable microbial composition were relatively weak (root biomass: r = 0.64 N.S., root C:N ratio: r = 0.64 N.S). Indirect paths through the latent variable soil structure varied in strength (root C:N ratio: r = 0.85, clay content: r = 0.52, root biomass: r = 0.17 N.S.). Soil structure influence on microbial composition (r = − 0.77 N.S.) was a stronger path than microbial composition influence on soil structure (r = 0.52 N.S.). Soil structure was the strongest direct path to microaggregate-within-macroaggregate C (r = 1.62), followed by root C:N ratio (r = − 0.85 N.S.), followed by microbial composition (r = − 0.14 N.S.), followed by root biomass (r = − 0.14 N.S.). Variance explained for physically sequestered soil C could not be evaluated because a negative variance was fit for that variable.

Discussion

Our results suggest that restoration age is a strong predictor of physically protected C measured by microaggregate-within-macroaggregate C stocks in temperate mesic perennial C_4 grasslands restored from long-term cultivation across three sites from cross-continental regions. Similar to many other studies, the accrual of physically protected C was linear on a decadal time scale but is expected to accrue at slower rates over time as a soil approaches C equilibrium (Jastrow 1996; Matamala et al. 2008; Baer et al. 2010). This linear increase was consistent with our hypothesis. The Scott et al. (2017) model was a good fit for northeast Kansas and northeast Free State, South Africa data, but contrary to our expectations the model was poor fit for southeast Nebraska and all sites combined. A poor model fits suggests that variables not measured in these studies are needed to adequately explain variance in microaggregate-within-macroaggregate C.

Predominant mechanisms that increase physically sequestered C in soil during restoration varied by chronosequence location. For example, northeast Kansas and northeast Free State, South Africa sites differed in the relative influence of root C:N, soil structure, and microbial composition on microaggregate-within-macroaggregate C. Root C:N ratio was more important in explaining variation in sequestered C in South Africa than Kansas. Recalcitrant root inputs with high C:N ratios positively correspond with sequestered C in the short term resulting from less C respired by microorganisms on an annual time scale (Robinson and Jacques 1958; Puget and Drinkwater 2001). Over a longer term, however, root inputs with lower C:N ratio are expected to promote microbial turnover and aggregation (Cotrufo et al. 2013). Soil structure was moderately important in models for both sites. Soil structure physically slows down oxidation of organic matter because of the arrangement of minerals (Six et al. 2000a, b). Microbial composition, especially PLFA biomass of AMF, had a large influence on accrual of protected C in Kansas, but not South Africa, which was unexpected and might be attributed to *Eragrostis curvula* being less dependent on mycorrhizal associations, as measured by mycorrhizal responsiveness, than *Sorghastrum nutans*, *Schizachyrium scoparium*, *Andropogon gerardii*, and *Panicum virgatum* (Wilson and Hartnett 1998).

Differences in soil texture and mean annual precipitation among the chronosequence locations could explain why roots contribute most strongly to accrual of physically sequestered C during grassland restoration in the South Africa chronosequence, but microbial composition (particularly AMF biomass) contribute most strongly in Kansas. Soil among the chronosequences varied slightly in clay content and percent clay was included in the SEM metamodel. There was likely not enough variation in clay content for this variable to emerge as an important causal influence of soil C accrual among soils with similar clay content. Climate could also cause variation in path strengths among regions by influencing plant belowground productivity and microbial biomass and composition (Zhao et al. 2016). Carbon stocks generally increase with precipitation (Klopfenstenin et al. 2015). The Kansas chronosequence had nearly 200 mm higher mean annual precipitation relative to South

Table 1 Fitted parameters from northeast Free State (NEFS) and northeast Kansas (NEKS) structural equation models

		NEFS				NEKS			
Response	Predictor	Estimate	Standard Error	Standardized Estimate	Intercept	Estimate	Standard Error	Standardized Estimate	Intercept
Soil structure	Macroaggregates	0.48	0.16	0.65	− 0.17	0.47	0.45	0.77	3.63
Soil structure	Bulk density	− 1.59	1.29	− 0.25	173.28	− 0.22	0.21	-0.71	13.26
Soil structure	Microaggregates-within-macroaggregates	2.35	0.76	0.70	43.12	0.16	0.15	0.68	3.79
Microbial composition	Microbial biomass C	0.18	0.29	0.15	1.96	0.39	0.11	0.74	0.75
Microbial composition	PLFA biomass	1.40	0.62	0.77	5.82	0.54	0.14	0.82	2.02
Microbial composition	AMF PLFA biomass	0.75	0.28	1.06	2.14	0.76	0.21	0.75	1.05
Microbial composition	Root biomass	0.75	0.39	0.64	0.00	0.72	0.43	0.41	0
Microbial composition	Root C:N	0.68	0.61	0.64	0.00	0.21	0.13	0.34	0
Microbial composition	Soil structure	− 0.38	0.32	− 0.77	0.00	2.29	1.95	2.29	0
Soil structure	Root biomass	0.39	0.68	0.17	0.00	2.99	2.92	0.72	0
Soil structure	Root C:N	1.84	0.69	0.85	0.00	0.44	0.47	0.34	0
Soil structure	Clay	0.18	0.06	0.52	0.00	NA	NA	NA	NA
Soil structure	Microbial composition	1.07	0.91	1.62	0.00	2.29	1.95	2.29	0
Physically Protected C	Root biomass	0.48	1.06	0.14	− 2.39	0.24	0.91	0.05	3.47
Physically Protected C	Root C:N	− 2.63	1.67	− 0.85	− 2.39	− 0.40	0.20	-0.29	3.47
Physically Protected C	Microbial composition	− 0.42	0.95	− 0.14	− 2.39	1.92	0.54	0.74	3.47
Physically Protected C	Soil structure	2.29	0.63	1.62	− 2.39	0.37	0.49	0.33	3.47

Units to use for predictions: bulk density = g cm^{-3}; PLFA biomass and AMF PLFA biomass = nmol g^{-1}, physically protected C, root biomass = g m^{-2}; macroaggregates, microaggregates-within-macroaggregates, and clay = %; root C:N = unitless. Note that PLFA biomass should include the AMF biomass when using the NEKS model (mesic silty soils), but AMF biomass should be excluded from PLFA biomass when using the NEFS model (arid sandy soils). Also note that all plant belowground biomass should be used (i.e., include rhizomes) for predictions using NEKS model, but only roots should be used for predictions from NEFS model

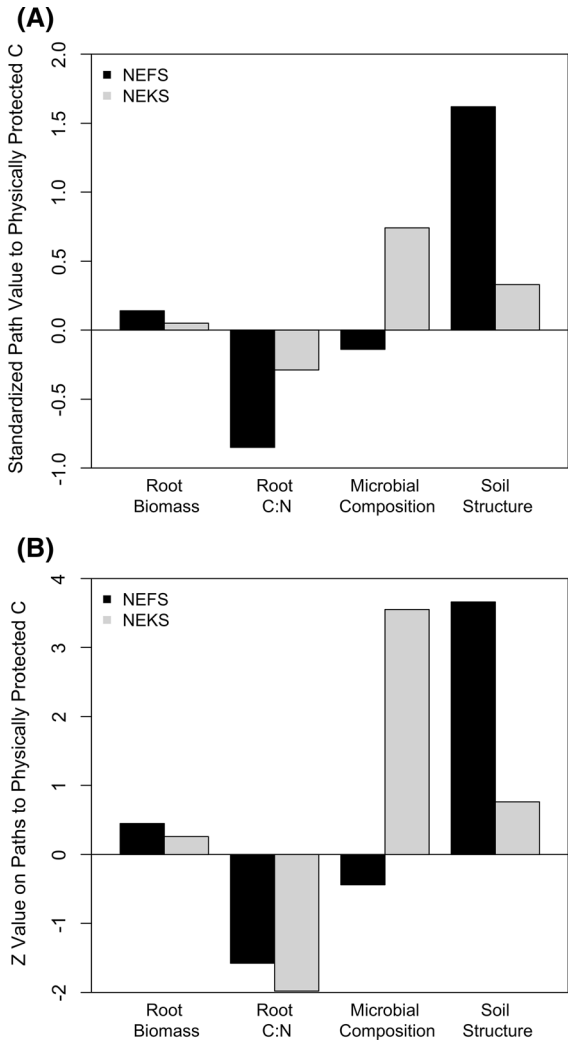

Fig. 4 Bar graphs of **a** standardized path values (i.e., relative influence of mechanism) and **b** Z values (unstandardized path value/standard error) of direct paths to physically protected carbon. *NEFS* northeast Free State; *NEKS* northeast Kansas

Africa, but we were unable to include climate variables in the models because they were measured at the site but not field level.

The difference in annual precipitation and slight difference in soil texture might explain the lack of strong influence of microbial composition (AMF biomass in particular) on sequestered C in South Africa. Root C:N ratio was similar between Kansas and South Africa, but Kansas restored soils had a higher concentration of PLFA AMF biomarkers (Table 2). Precipitation and AMF biomarker abundance are consistent with the previous finding that higher mean precipitation results in more AMF hyphae (Zhang et al. 2016). Clay content and AMF biomarker abundance (Table 2) are consistent with previous findings that AMF abundance is associated with clay content in disturbed ecosystems (Xue et al. 2018) and grasslands specifically (Kotzé et al. 2017). Clayey grassland soils have more soil C in several fractions, regardless of climate (Loke et al. 2020). Differences in NEFS and NEKS are also consistent with the finding that fungi are less important for soil aggregates in clayey soils (De Gryze et al. 2005).

In the cases where our model did not fit well, i.e., southeast Nebraska and all sites combined, measuring additional variables may be needed to explain variance in microaggregate-within-macroaggregate C. Clay-organic matter interactions such as adsorption may be a larger store of C in clayey soils, especially those dominated by 2:1 clay minerals, such as smectites. Smectite group clay minerals, which dominated the soils in southeast Nebraska, promote organic matter accumulation between the layers of their microcrystals (interlayer complex formation) as well as between the smectite minerals due to high surface area and charge (Theng 1974, 1979). Another potential explanation is that not all organic C was complexed to clay minerals causing less dispersion of clay minerals upon wetting (Dexter et al. 2008; Klopfenstein et al. 2015), but the C stocks were small enough (C:clay ratio < 0.1) that this behavior is unexpected. Entrainment of soil C within carbonates might also explain lack of model fit, though soil was sampled above the depth where carbonates generally accumulate, and carbonates are likely less than 6% of total C in all sites. As such, dominance of smectite minerals is the most likely explanation for lack of model fit in Nebraska. Additional variables that could influence microaggregate-within-macroaggregate C and deserve consideration in future modeling studies include black carbon (carbon that has been partially combusted; Ding et al. 2017; Melas et al. 2017) and inorganic N deposition (Field et al. 2017). Black carbon can potentially increase aggregation and thereby increase physical protection of soil organic matter (Wang et al. 2017). High inorganic N deposition could also slow decomposition of organic C through a decline in lignolytic exoenzymes (Zak et al. 2008). Additional indicators of microbial composition such as C degrading enzyme potentials could make model matrices symmetric and all eigenvalues positive (positive definite), possibly allowing accurate

Table 2 Comparison of estimated marginal means and associated standard errors of soil properties among northeast Free State, RSA (NEFS) and northeast Kansas, USA (NEKS), and southeast Nebraska, USA (SENE)

	Clay (%)	Root C:N	MBC (μg g^{-1})	Total PLFA (nmol g^{-1})	AMF PLFA (nmol g^{-1})
NEFS	17.2 ± 1.3 b	73.7 ± 3.5 b	192.0 ± 32.7 b	53.4 ± 3.6 ab	2.0 ± 0.2 a
NEKS	29.8 ± 2.1 a	70.7 ± 5.3 a	152.6 ± 12.1 b	42.8 ± 5.9 b	3.9 ± 0.4 a
SENE	32.9 ± 1.4 a	73.7 ± 3.5 a	648.1 ± 34.9 a	65.8 ± 4.1 a	3.0 ± 0.2 b

All variables in the table had a significant ANOVA ($P < 0.05$). Letters refer to least significant differences contrasts

MBC microbial biomass C; *PLFA* phospholipid fatty acid biomass; *AMF* arbuscular mycorrhizal fungi

estimation of the amount of variance explained (coefficients of determination). Because sites vary in amount of clay and clay mineralogy, we encourage further examination of interactive effects of clay with known mechanisms of physically sequestered soil C.

Conclusions

Across all sites, physically protected C was sequestered at a rate of 16 ± 5 g m^{-2} $year^{-1}$, nearly the same rate as total C accrual (18 ± 7 g m^{-2} $year^{-1}$), during grassland restoration within the decadal timeframe when C accrual rates are linear, representing a generalized ecosystem service provided by grassland restoration on soils with 10–30% clay content. If carbonates were not equally distributed among aggregate fractions, this comparison of physically protected C and total C could be misleading. The estimates for carbon accrual only apply to restoration of fields that were in long-term cultivation, such that a lower equilibrium of soil C was approached (i.e., long-term cultivation substantially lowered the soil's capacity to sequester C). The physically protected and total soil C accrual rates are an order of magnitude higher than soil organic C accrual rates from conversion to reduced tillage in corn-soybean rotations (1.6 g C m^{-2} $year^{-1}$; Yu et al. 2020). The microaggregate-within-macroaggregate fraction is where most C accumulated, suggesting this fraction is diagnostic of C sequestration in grasslands. This fraction was also identified as a diagnostic fraction of C sequestration in agricultural soils (Six and Paustian 2014). Our analysis demonstrates that accrual of physically protected soil C can be accurately predicted by root biomass, root C:N ratio, soil structure (bulk density, percent of macroaggregates on a per whole soil mass basis, percent of microaggregate-within-macroaggregates on a per macroaggregate mass basis), and microbial composition (microbial biomass C, total PLFA biomass, and PLFA AMF biomass) for soils with a clay content greater than ∼ 10% and less than ∼ 30%. Further, this study suggests that accrual of physically protected soil C might be driven primarily by root inputs in arid climates with sandy loam soils but by microbial composition in mesic climates with silt loam soils.

Acknowledgements Amanda Rothert assisted with lab analyses.

Funding No funding was provided for this synthesis work.

Data availability Data used in this synthesis is available through the Environmental Data Initiative repository: https://doi.org/10.6073/pasta/6f05427623092f016cdf696d8c99c5cb. The dataset (before averaging to plot level) from the northeast Kansas, USA site (Scott et al. 2017) is included as electronic supplementary material. A site map of the northeast Kansas chronosequence is also included as electronic supplementary material.

Code availability R code is available through the Environmental Data Initiative repository: https://doi.org/10.6073/pasta/6f05427623092f016cdf696d8c99c5cb.

Declarations

Conflict of interest The authors declare no conflict of interest.

References

Angers D, Caron J (1998) Plant induced changes in soil structure: processes and feedbacks. Biogeochemistry 42:55–72

Bach EM, Baer SG, Meyer CK, Six J (2010) Soil texture affects soil microbial and structural recovery during grassland restoration. Soil Biol Biochem 42:2182–2191

Baer SG, Birge H (2019) Soil ecosystem services: an overview. In: Reicosky D (ed) Managing soil health for sustainable agriculture. Burleigh Dodds Science Publishing Limited, Cambridge

Baer SG, Kitchen DJ, Blair JM, Rice CW (2002) Changes in ecosystem structure and function along a chronosequence of restored grasslands. Ecol Appl 12:1688–1701

Baer SG, Blair JM, Collins SL, Knapp AK (2003) Soil resources regulate productivity and diversity in newly established tallgrass prairie. Ecology 84:724–735

Baer SG, Meyer CK, Bach EM, Klopf RP, Six J (2010) Contrasting ecosystem recovery on two soil textures: implications for carbon mitigation and grassland conservation. Ecosphere 1:article 5

Baer SG, Bach EM, Meyer CK, Du Preez CC, Six J (2015) Restoration of cultivated soil in the Free State (South Africa) and comparison to Nebraska (United States) provides a global perspective of belowground ecosystem recovery in response to grassland restoration. Ecosystems 18:390–403

Bartoń K (2018) MuMIn: multi-model inference. R package version 1.40.4

Bates D, Maechler M, Bolker B, Walker S (2015) Fitting linear mixed-effects models using lme4. J Stat Softw 67:1–48

Bligh EG, Dyer WJ (1959) A rapid method of total lipid extraction and purification. Can J Biochem Physiol 37:911–917

Bossio DA, Scow KM, Gunapala N, Graham KJ (1998) Determinants of soil microbial communities: effects of agricultural management, season, and soil type on phospholipid fatty acid profiles. Microb Ecol 36:1–12

Canty A, Ripley B (2017) Boot: bootstrap R (S-Plus) functions. R package version 1.3–20

Cotrufo MF, Wallenstein MD, Boot CM, Denef K, Paul E (2013) The Microbial Efficiency-Matrix Stabilization (MEMS) framework integrates plant litter decomposition with soil organic matter stabilization: do labile plant inputs form stable soil organic matter? Glob Change Biol 19:988–995

Davidson AC, Hinkley DV (1997) Bootstrap methods and their applications. Cambridge University Press, Cambridge

DeGrood SH, Claassen VP, Scow KM (2005) Microbial community composition on native and drastically disturbed serpentine soils. Soil Biol Biochem 37:1427–1435

De Gryze S, Six J, Brits C, Merckx R (2005) A quantification of short-term macroaggregate dynamics: influences of wheat residue input and texture. Soil Biol Biochem 37:55–66

Denef K, Six J, Merckx R, Paustian K (2004) Carbon sequestration in microaggregates of no-tillage soils with different clay mineralogy. Soil Sci Soc Am J 68:1935–1944

Denef K, Zotarelli L, Boddey RM, Six J (2007) Microaggregate-associated carbon as a diagnostic fraction for management-induced changes in soil organic carbon in two Oxisols. Soil Biol Biochem 39:1165–1172

Dexter AR, Richard G, Arrouays D, Czyż EA, Jolivet C, Duval O (2008) Complexed organic matter controls soil physical properties. Geoderma 144:620–627

Ding Y, Liu YG, Liu SB, Huang XX, Li ZW, Tan XF, Zeng GM, Zhou L (2017) Potential benefits of biochar in agricultural soils: a review. Pedosphere 27:645–661

Du Toit ME, Du Preez CC, Hensley M, Bennie ATP (1994) Effect of cultivation on the organic matter content of selected dryland soils in South Africa. S Afr J Plant Soil 11:71–79

Ehrenfeld JG, Ravit B, Elgersma K (2005) Feedback in the plant–soil system. Annu Rev Environ Resour 30:75–115

Elliot ET, Coleman DC, Ingrahm RE, Trofymow JA (1984) Carbon and energy flow through microflora and microfauna in the soil subsystem of terrestrial ecosystems. In: Klug MJ, Reddy CA (eds) Current perspectives in microbial ecology. American Society for Microbiology, Washington, D.C., pp 424–433

Field CD, Evans CD, Dise NB, Hall JR, Caporn SJM (2017) Long-term nitrogen deposition increases heathland carbon sequestration. Sci Total Environ 592:426–435

Gale WJ, Cambardella CA, Bailey TB (2000) Root-derived carbon andthe formation and stabilization of aggregates. Soil Sci Soc Am J 64:201–207

Grace JB (2006) Structural equation modeling and natural systems. Cambridge University Press, Cambridge

Jastrow JD (1996) Soil aggregate formation and the accrual of particulate and mineral-associated organic matter. Soil Biol Biochem 28:665–676

Klopfenstein ST, Hirmas DR, Johnson WC (2015) Relationships between soil organic carbon and precipitation along a climosequence in loess-derived soils of the Central Great Plains, USA. Catena 133:25–34

Kong AYY, Six J, Bryant DC, Denison RF, van Kessel C (2005) The relationship between carbon input, aggregation, and soil organic carbon stabilization in sustainable cropping systems. Soil Sci Soc Am J 69:1078–1085

Kotzé E, Sandhage-Hofmann A, Amelung W, Oomen RJ, du Preez CC (2017) Soil microbial communities in different rangeland management systems of a sandy savanna and clayey grassland ecosystem, South Africa. Nutr Cycl Agroecosyst 107:227–245

Kuznetsova A, Brockhoff PB, Christensen RHB (2016) lmerTest: tests in linear mixed effects models. R package version 2.0–33

Lee J, Hopmans JW, Rolston DE, Baer SG, Six J (2009) Determining soil C stock changes: simple bulk density corrections fail. Agric Ecosyst Environ 134:251–256

Lenth R (2020) Emmeans: estimated marginal means, aka least-squares means. R package version 1.4.6

Lobe I, Amelung W, Du Preez CC (2001) Losses of soil carbon and nitrogen with prolonged arable cropping from soils of the South African Highveld. Eur J Soil Sci 52:93–101

Lobe I, Du Preez CC, Amelung W (2002) Influence of prolonged arable cropping on lignin compounds in sandy soils of the South African Highveld. Eur J Soil Sci 53:553–562

Loke PF, Kotzé E, Du Preez CC, Twigge L (2020) Cross-rangeland comparisons on soil carbon dynamics in the *pedoderm* of semi-arid and arid South African commercial farms. Geoderma 381:114689

Matamala R, Jastrow JD, Miller RM, Garten CT (2008) Temporal changes in C and N stocks of restored prairies: implications for C sequestration strategies. Ecol Appl 18:1470–1488

McLauchlan K (2006) The nature and longevity of agricultural impacts on soil carbon and nutrients: a review. Ecosystems 9:1364–1382

Melas GB, Ortiz O, Alacaniz JM (2017) Can biochar protect labile organic matter against mineralization in soil? Pedosphere 27:822–831

Newman EI (1985) The rhizosphere: carbon sources and microbial populations. In: Fitter AH (ed) Ecological interactions in soil: plants, microbes and animals. Special Publication of the British Ecological Society 4. Blackwell Scientific, Oxford, pp 107–121

Paustian K, Andren O, Janzen HH, Lal R, Smith P, Tian G, Tiessen H, Van Noordwijk M, Woomer PL (1997) Agricultural soils as a sink to mitigate CO_2 emissions. Soil Use Manag 13:230–244

Puget P, Drinkwater LE (2001) Short-term dynamics of root- and shoot- derived carbon from a leguminous green manure. Soil Sci Soc Am J 65:771–779

R Core Team (2016) R: a language and environment for statistical computing. R Foundation for Statistical Computing, Vienna

Robinson GS, Jacques WA (1958) Root development in some common New Zealand pasture plants. New Zeal J of Agr Res 1:199–216

Rosenzweig ST, Carson MA, Baer SG, Blair JM (2016) Changes in soil properties, microbial biomass, and uxes of C and N in soil following post-agricultural grassland restoration. Appl Soil Ecol 100, 186–194. https://doi.org/10.1016/j.apsoil.2016.01.001

Rosseel Y (2012) Lavaan: an R package for structural equation modeling. J Stat Softw 48:1–36

Scott NA (1998) Soil aggregation and organic matter mineralization in forests and grasslands: plant species effects. Soil Sci Soc Am J 62:1081–1089

Scott DA, Baer SG, Blair JM (2017) Recovery and relative influence of root, microbial, and structural properties of soil on physically sequestered carbon stocks in restored grassland. Soil Sci Soc Am J 81:50–60

Scott DA, Rosenzweig ST, Baer SG, Blair JM (2019) Changes in potential nitrous oxide efflux during grassland restoration. J Environ Qual 48:1913–1917

Simpson RT, Frey SD, Six J, Thiet RK (2004) Preferential accumulation of microbial carbon in aggregate structures of no-tillage soils. Soil Sci Soc Am J 68:1249–1255

Six J, Paustian K (2014) Aggregate-associated soil organic matter as an ecosystem property and a measurement tool. Soil Biol Biochem 68:A4–A9

Six J, Paustian K, Elliott ET, Combrink C (2000a) Soil structure andorganic matter: I. Distribution of aggregate-size classes and aggregate-associated carbon. Soil Sci Soc Am J 64:681–689

Six J, Elliot ET, Paustian K (2000b) Soil macroaggregate turnover and microaggregate formation: a mechanism for C sequestration under no-tillage agriculture. Soil Biol Biochem 32:2099–2103

Six J, Feller C, Denef K, Ogle SM, de Moraes Sa JC, Albrecht A (2002) Soil organic matter, biota and aggregation in temperate and tropical soils—effects of no-tillage. Agronomie 22:755–775

Six J, Bossuyt H, Degryze S, Denef K (2004) A history of research onthe link between (micro)aggregates, soil biota, and soil organic matterdynamics. Soil Tillage Res 79(1):7–31

Smith AP, Marín-Spiota E, de Gra MA, Balser TC (2014) Microbial community structure varies across soil organic matter aggregate pools during tropical land cover change. Soil Biol Biochem 77:292–303

Smucker AJM, Safir GR (1986) Root and soil microbial interactions which influence the ability to photoassimilate carbon to the rhizosphere. In: Mitchell MJ, Nakas JP (eds) Micro oral and faunal interactions in natural and agroecosystems. Junk Publishers, Dordrecht, pp 203–244

Stewart CE, Paustian K, Conant RT, Plante AF, Six J (2007) Soil carbon saturation: concept, evidence and evaluation. Biogeochemistry 86:19–31

Theng BKG (1974) The chemistry of clay-organic reactions. Hilger, London

Theng BKG (1979) Formation and properties of clay-polymer complexes. Elsevier, Amsterdam

Tisdall JM, Oades JM (1982) Organic matter and waterstable aggregates in soils. J Soil Sci 33:141–163

USDA National Cooperative Soil Survey (2008) Wymore series. USDA National Cooperative Soil Survey, Waverly

USDA National Cooperative Soil Survey (2020) Arispe series. USDA National Cooperative Soil Survey, Waverly

Wang D, Fonte S, Parikh SJ, Six J, Scow KM (2017) Biochar additions can enhance soil structure and the physical stabilization of C in aggregates. Geoderma 303:110–117

Wilson GWT, Hartnett DC (1998) Interspecific variation in plant responses to mycorrhizal colonization in tallgraaa prairie. Am J Bot 85:1732–1738

Wilson GWT, Rice CW, Rillig MC, Springer A, Hartnett DC (2009) Soil aggregation and carbon sequestration are tightly correlated with the abundance of arbuscular mycorrhizal fungi: results from long-term field experiments. Ecol Lett 12:452–461

Xue P-P, Carrillo Y, Pino V, Minansy B, McBratney AB (2018) Soil properties drive microbial community structure in a large scale transect in South Eastern Australia. Sci Rep 8:11725

Yu Z, Lu C, Hennessy DA, Feng H, Tian H (2020) Impacts of tillage practices on soil carbon stocks in the US corn-soybean cropping system during 1998 to 2016. Environ Res Lett 15:014008

Zak DR, Holmes WE, Burton AJ, Pregitzer KS, Talhelm AF (2008) Simulated atmospheric NO_3^- deposition increases soil organic matter by slowing decomposition. Ecol Appl 18:2016–2027

Zhang J, Wang F, Che R, Wang P, Liu H, Ji B, Cui X (2016) Precipitation shapes communities of arbuscular mycorrhizal fungi in Tibetan alpine steppe. Sci Rep 6:23488

Zhao C, Miao Y, Yu C, Zhu L, Wang F, Jiang L, Hui D, Wan S (2016) Soil microbial community composition and respiration along an experimental precipitation gradient in a semiarid steppe. Sci Rep 6:24317

Terms and Conditions

Springer Nature journal content, brought to you courtesy of Springer Nature Customer Service Center GmbH (“Springer Nature”).
Springer Nature supports a reasonable amount of sharing of research papers by authors, subscribers and authorised users (“Users”), for small-scale personal, non-commercial use provided that all copyright, trade and service marks and other proprietary notices are maintained. By accessing, sharing, receiving or otherwise using the Springer Nature journal content you agree to these terms of use (“Terms”). For these purposes, Springer Nature considers academic use (by researchers and students) to be non-commercial.
These Terms are supplementary and will apply in addition to any applicable website terms and conditions, a relevant site licence or a personal subscription. These Terms will prevail over any conflict or ambiguity with regards to the relevant terms, a site licence or a personal subscription (to the extent of the conflict or ambiguity only). For Creative Commons-licensed articles, the terms of the Creative Commons license used will apply.
We collect and use personal data to provide access to the Springer Nature journal content. We may also use these personal data internally within ResearchGate and Springer Nature and as agreed share it, in an anonymised way, for purposes of tracking, analysis and reporting. We will not otherwise disclose your personal data outside the ResearchGate or the Springer Nature group of companies unless we have your permission as detailed in the Privacy Policy.
While Users may use the Springer Nature journal content for small scale, personal non-commercial use, it is important to note that Users may not:

1. use such content for the purpose of providing other users with access on a regular or large scale basis or as a means to circumvent access control;
2. use such content where to do so would be considered a criminal or statutory offence in any jurisdiction, or gives rise to civil liability, or is otherwise unlawful;
3. falsely or misleadingly imply or suggest endorsement, approval , sponsorship, or association unless explicitly agreed to by Springer Nature in writing;
4. use bots or other automated methods to access the content or redirect messages
5. override any security feature or exclusionary protocol; or
6. share the content in order to create substitute for Springer Nature products or services or a systematic database of Springer Nature journal content.

In line with the restriction against commercial use, Springer Nature does not permit the creation of a product or service that creates revenue, royalties, rent or income from our content or its inclusion as part of a paid for service or for other commercial gain. Springer Nature journal content cannot be used for inter-library loans and librarians may not upload Springer Nature journal content on a large scale into their, or any other, institutional repository.
These terms of use are reviewed regularly and may be amended at any time. Springer Nature is not obligated to publish any information or content on this website and may remove it or features or functionality at our sole discretion, at any time with or without notice. Springer Nature may revoke this licence to you at any time and remove access to any copies of the Springer Nature journal content which have been saved.
To the fullest extent permitted by law, Springer Nature makes no warranties, representations or guarantees to Users, either express or implied with respect to the Springer nature journal content and all parties disclaim and waive any implied warranties or warranties imposed by law, including merchantability or fitness for any particular purpose.
Please note that these rights do not automatically extend to content, data or other material published by Springer Nature that may be licensed from third parties.
If you would like to use or distribute our Springer Nature journal content to a wider audience or on a regular basis or in any other manner not expressly permitted by these Terms, please contact Springer Nature at

onlineservice@springernature.com